The role of quantum confinement and crystalline structure on excitonic lifetimes in silicon nanoclusters

L. J. Borrero-González,[1,a)] L. A. O. Nunes,[1] M. R. B. Andreeta,[1] J. Wojcik,[2] P. Mascher,[2] Y. A. Pusep,[1] D. Comedi,[3] and F. E. G. Guimarães[1]

[1]*Instituto de Física de São Carlos, Universidade de São Paulo, CP 369, 13560-970 São Carlos, SP, Brazil*

[2]*Department of Engineering Physics, CEDT, McMaster University, Hamilton, Ontario L8S 4L7, Canada*

[3]*Dep. Física, LAFISO and CONICET, FACET, Universidad Nacional de Tucumán, Av. Independencia 1800, 4000 Tucumán, Argentina*

(Received 9 March 2010; accepted 2 June 2010; published online 8 July 2010)

The emission energy dependence of the photoluminescence (PL) decay rate at room temperature has been studied in Si nanoclusters (Si-ncl) embedded in Si oxide matrices obtained by thermal annealing of substoichiometric Si oxide layers Si_yO_{1-y}, y=(0.36,0.39,0.42), at various annealing temperatures (T_a) and gas atmospheres. Raman scattering measurements give evidence for the formation of amorphous Si-ncl at T_a=900 °C and of crystalline Si-ncl for T_a=1000 °C and 1100 °C. For T_a=1100 °C, the energy dispersion of the PL decay rate does not depend on sample fabrication conditions and follows previously reported behavior. For lower T_a, the rate becomes dependent on fabrication conditions and less energy dispersive. The effects are attributed to exciton localization and decoherence leading to the suppression of quantum confinement and the enhancement of nonradiative recombination in disordered and amorphous Si-ncl. © *2010 American Institute of Physics*. [doi:10.1063/1.3457900]

I. INTRODUCTION

A large variety of Si nanostructures have been extensively studied in the past few years due to their potential applications in Si-based light-emitting devices. A technologically important structure, which is fully complementary metal-oxide semiconductor (CMOS) compatible and takes advantage of the well-known good passivation and stability of the Si/SiO_2 interface, consists of crystalline silicon nanoclusters (Si-ncl) dispersed in an amorphous SiO_2 matrix.[1,2] The mechanisms of light emission in these structures have been studied intensively. Time-resolved photoluminescence (PL) measurements have shown a nonexponential PL intensity decay in the microsecond range that can be fit by the stretched-exponential function $I(t)=I_0 \exp[-(t/\tau)^{\beta}]$, where I_0 is the initial PL intensity, τ is a lifetime, and $\beta \leq 1$ is a dispersion exponent.[3,4] Initially, it was suggested that the nonexponential behavior was due to exciton hopping effects combined with Si-ncl size variations within a sample.[5] Interestingly, however, it has been observed in virtually all Si nanostructures studied, ranging from porous silicon[5] to size selected Si-ncl ensembles.[6] Furthermore, the PL decay rates ($1/\tau$) have often been seen to increase exponentially with increasing PL emission energy according to

$$\frac{1}{\tau} = Ae^{(E/E_0)}, \quad (1)$$

where A is a constant, E is the PL emission energy, and E_0 is a characteristic energy. To explain such a "universal" behavior, Delerue *et al.*[6] proposed a model that considered the inherent character of quantum confined excitons in indirect gap nanostructures. This model predicted E_0=0.31 eV, in close agreement with the reported typical experimental values[3–6] of E_0=0.3 eV. However, there has been a long standing debate on the role of the Si/SiO_2 interface states in the recombination process and the luminescence from Si-ncl/SiO_2 materials. Moreover, the quantum confinement (QC) mechanism itself has been questioned.[7] In addition, the role of the Si-ncl structure, which may be strongly disordered or even amorphous, is not well understood. Most studies have focused mainly on systems with Si-ncl possessing high degree of crystallinity. Only sparse work has been directed to disordered or amorphous Si-ncl that may be obtained, for instance, by annealing substoichiometric Si oxide layers at relatively low temperatures (<1100 °C).

In this work, we focus on the influence of varying Si-ncl structures on PL decay rates from Si-ncl embedded in amorphous Si oxides. In contrast to previous findings, we obtain E_0 values much larger than 0.3 eV that depend strongly on the fabrication conditions [i.e., the Si concentration in the Si oxide, the annealing temperature (T_a), and gas atmosphere]. We propose that strong Si-ncl lattice distortion is at the origin of this effect.

II. EXPERIMENTAL DETAILS

The Si_yO_{1-y} films were deposited on fused quartz substrates using an electron cyclotron resonance-plasma enhanced chemical vapor deposition system described elsewhere.[8] The Si contents (y) were 0.36, 0.39, and 0.42, determined as reported previously.[9] The annealing of the films was performed in a quartz tube furnace under either Ar or Ar+5%H_2 atmospheres for 2 h and at temperatures of 900, 1000, and 1100 °C. These conditions lead to Si-ncl at

a)Electronic mail: lborrero@ursa.ifsc.usp.br

 © 2010 American Institute of Physics

Author complimentary copy. Redistribution subject to AIP license or copyright, see http://jap.aip.org/jap/copyright.jsp

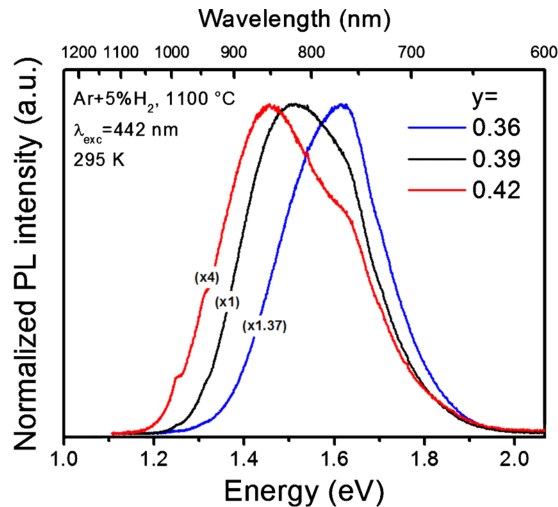

FIG. 1. (Color online) Room-temperature PL spectra for samples with y $=0.36, 0.39, 0.42$ (blue, black, and red lines, respectively) annealed under $Ar+5\%H_2$ at 1100 °C. The excitation wavelength was 442 nm.

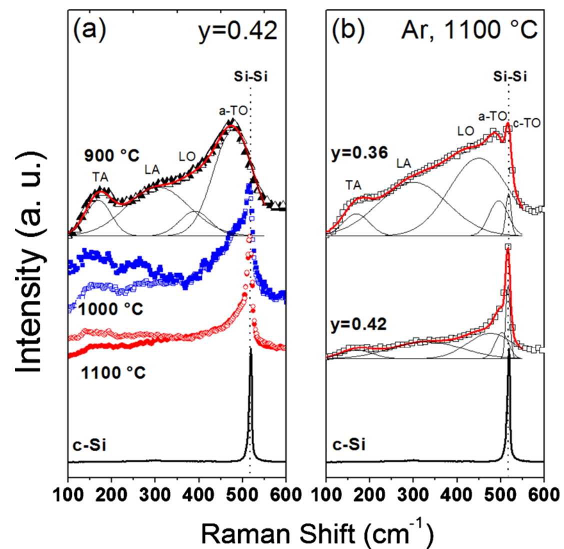

FIG. 2. (Color online) (a) Raman spectra for the samples with y=0.42 annealed at 900, 1000, and 1100 °C (triangle, square, and circle, respectively) under Ar (full symbols), and $Ar+5\%H_2$ (empty symbols). (b) Raman spectra for the samples with Si content y=(0.36,0.42) annealed at 1100 °C under Ar. The Raman spectrum for the c-Si is included in both graphs. The red lines are the Gaussian fits.

various stages of formation and Si-ncl/SiO_2 interface defect passivation. The PL peaks that redshift in the 700–900 nm region with increasing Si-ncl mean size, as can be seen in Fig. 1 for samples with y=0.36,0.39,0.42 (blue, black, and red lines, respectively) annealed under $Ar+5\%H_2$ at 1100 °C, in qualitative agreement with the proposed excitonic QC mechanism of light emission.[9,10]

The optical properties of the Si-ncl were studied by using PL, confocal Raman, and time-resolved PL spectroscopies. All measurements were made at room temperature. The PL spectra were recorded by using an HR4000 Ocean Optics spectrometer as a detection system. The 442 nm line of a He–Cd laser was used as the excitation source. In the Raman studies, an argon-ion laser excitation line (514.5 nm) was used. The decay kinetics of the luminescence were studied using the second harmonic of a Q-switch neodymium-doped yttrium aluminium garnet (Nd:YAG) laser (532 nm, 6 Hz repetition rate) as the source of excitation. The excitation pulse width was 5 ns. The decay luminescence was detected by a Thermo Jarrel Ash monochromator (25 cm focal length) equipped with a Hamamatsu R928 photomultiplier tube. A digital oscilloscope processed the signal averaging over 250 pulses.

III. RESULTS AND DISCUSSIONS

Figure 2(a) shows Raman spectra for the six samples with y=0.42 and thermal annealed at 900, 1000, and 1100 °C (triangles, squares, and circles, respectively) and under Ar (full symbols) and $Ar+5\%H_2$ (empty symbols). By performing a multiple Gaussian fit from 100 to 550 cm^{-1}, the TA, LA, LO, and TO phonon modes of amorphous silicon (a-Si), located at around 170 cm^{-1}, 300 cm^{-1}, 400 cm^{-1}, and 480 cm^{-1}, respectively, can be deduced for the samples annealed at 900 °C. The solid line represents the Gaussian fit. All spectra were normalized to the TO phonon mode. These modes are still present for samples annealed at 1000 and 1100 °C. However, an additional mode appears near 516 cm^{-1} associated to the TO phonon mode of c-Si, indicating crystallization processes of the amorphous phase.[11] In addition, the Si–Si Raman peak for Si-nc is downshifted (by ~ 2 cm^{-1}) as compared to the measured Raman position in perfect c-Si (518.5 cm^{-1}) in the absence of disorder and stress effects[12] [see dotted vertical line in Fig. 2(a)]. The Raman spectra have nearly the same line shape for the series of samples prepared under Ar and $Ar+5\%H_2$ with the same annealing temperatures. Figure 2(b) compares Raman spectra for the Si_yO_{1-y} samples with y=0.36 and 0.42 and $T_a=1100$ °C under Ar. Again, the Si–Si mean peak is positioned 2 cm^{-1} below the wave number expected for bulk Si, indicating phonon confinement effect,[13] while the line width remains at 11 cm^{-1}. The major vibrational features of a-Si are also present in the Raman spectra for these two samples. Note that the Si–Si peak intensity decreases when the Si content (y) is reduced indicating that the density and the size of Si-ncl decreases with the reduction in y. In addition, it is found that for the amorphous contribution, the integrated area diminishes, the linewidth narrows, and the peak position blueshifts when T_a or y increase. This is probably due to the phonon confinement effect in the a-Si phase, similar to the case of crystalline Si-ncl.[11] The crystalline fraction defined as $F_c=I_c/(I_c+\alpha I_a)$, where $\alpha=0.8$ is the Raman cross section ratio for phonon excitation of c-Si crystalline (I_c) to the amorphous (I_a) components[14] increase for increasing T_a or y (see Tables I and II).

TABLE I. Crystalline fractions for the samples with Si content y =(0.36,0.42) annealed at 1100 °C under Ar.

Silicon content, y	Crystalline Fraction, F_c (%)
0.36	30 ± 2
0.42	41 ± 1

Author complimentary copy. Redistribution subject to AIP license or copyright, see http://jap.aip.org/jap/copyright.jsp

TABLE II. Crystalline fractions for the samples with Si content y=0.42, annealed at 900, 1000, and 1100 °C under Ar+5%H_2.

Annealing temperature, T_a (°C)	Crystalline Fraction, F_c (%)
900	0
1000	39±2
1100	53±1

Figure 3(a) shows the PL decay curves from the Si_yO_{1-y} samples with y=0.42 recorded at E_{det}=1.47 eV, for T_a =900, 1000, and 1100 °C (triangle, square, and circle, respectively) annealed under Ar (full symbols) and Ar +5%H_2 (empty symbols). The decay behavior of the laser excitation pulse is also shown. Lines are fits of the stretched-exponential function to the experimental data, from which the β values were determined for each sample. It can be seen that a satisfactory fit is obtained and that for the same gas atmosphere, samples annealed at high temperatures show slow kinetics when compared with samples annealed at low temperatures. In addition, for fixed T_a, the decay is slower for hydrogenated samples when compared with nonhydrogenated ones. This could be explained by passivation of the Si-ncl surface when hydrogen is used, eliminating nonradiative centers, such as Si dangling bonds. Figure 3(b) shows the emission energy dependence of PL decay rates for the same samples as in Fig. 3(a). At first observation, $1/\tau$ is exponentially dependent on emission energy, $1/\tau \propto \exp(E/E_0)$, in agreement with Eq. (1). Moreover, this behavior is obeyed for all T_a and both gas atmospheres used in the annealing treatments. For samples with y=(0.36,0.39) we have observed the same dependence, however E_0 increases with decreasing T_a. Figure 4 shows the emission energy dependence of PL decay rates for samples with different Si content (y=0.36,0.39,0.42—triangle, circle, and square, respectively) and annealed at 1100 °C under Ar. The behavior expected from Eq. (1) is seen to be obeyed in all cases except for y=0.36 at low detection energy, where the PL decay rates level off. In addition, E_0 increases and the decay rates decrease with decreasing Si content.

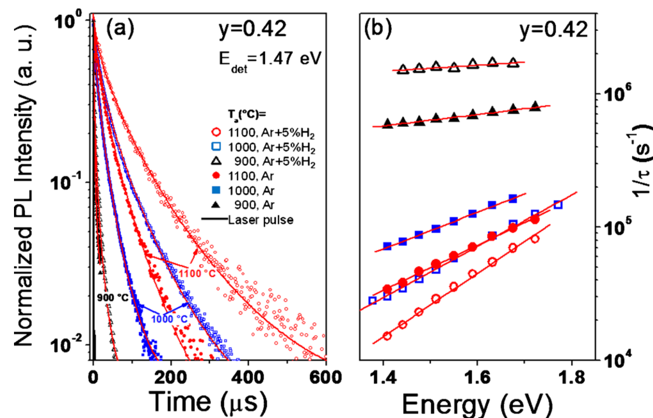

FIG. 3. (Color online) (a) PL decay curves of Si-ncl measured at E_{det} =1.47 eV for y=0.42. Triangles, squares, and circles corresponds to T_a =900, 1000, and 1100 °C. Empty (full) symbols corresponds to hydrogenated (nonhydrogenated) samples. Lines are linear fit by using the stretched-exponential function. The laser pulse is also shown. (b) Dependence of PL decay rates on observation energy for the same samples in (a). Solid lines correspond to a linear fit by using Eq. (1).

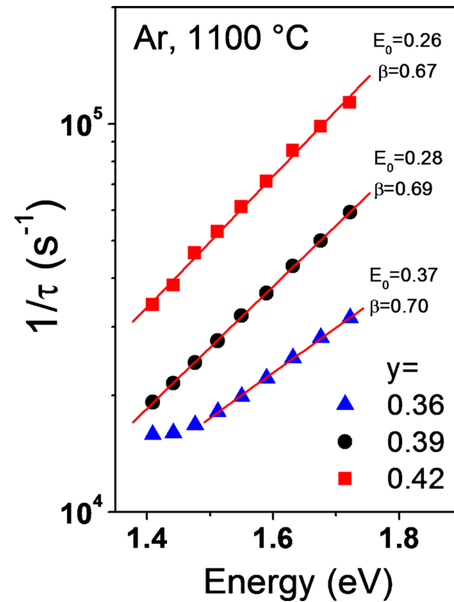

FIG. 4. (Color online) The observation energy dependence of PL decay rates at room temperature for samples with different Si content y =(0.36,0.39,0.42-triangle,circle,and square,respectively) and annealed at 1100 °C under Ar. Solid lines correspond to a linear fit by using Eq. (1).

These results are qualitatively similar to those reported by Pavesi[5] for porous Si, except for the fact that here the E_0 parameter is not constant for samples prepared under different conditions. Garcia *et al.*[15] studied crystalline Si-ncl embedded in SiO_2 and observed almost no dependence of the PL lifetime on Si content. More recently, Derr *et al.*[4] also observed the same dependence as in Eq. (1), with E_0 =0.3 eV for different crystalline Si-ncl sizes.

Hence, in contrast to previous experimental reports on similar systems, our results show a clear dependence of the emission energy dependent PL decay rate, namely the E_0 parameter, on the fabrication conditions. We propose that this dependence is due to the effect of Si-ncl lattice disorder, and eventually Si-ncl amorphicity, on QC and recombination kinetics. To explain the physics behind the empirical dependence of $1/\tau$ on the emission energy [Eq. (1)], Delerue *et al.*[6] performed combined tight-binding/valence force-field calculations of phonon-assisted optical transition matrix elements that are expected in an indirect band gap material such as Si. In this model, the effect of QC, namely electron and hole wave function broadening in k-space leading to increasing probability for zero-phonon transitions,[16] was taken into account automatically through the electronic structure calculation in the tight-binding approach. The strong emission energy dispersion of the PL rate is then a result of the increasing electron-hole wave function overlap in k-space, which is larger at larger emission energy and affects both zero-phonon and phonon-assisted transitions.[6] Therefore, the strong emission energy dispersion of the PL decay rate emerges as result of the indirect character of the Si band gap and the QC effects on the radiative transition rates, which increase with increasing emission energy (i.e., smaller Si-ncl

Author complimentary copy. Redistribution subject to AIP license or copyright, see http://jap.aip.org/jap/copyright.jsp

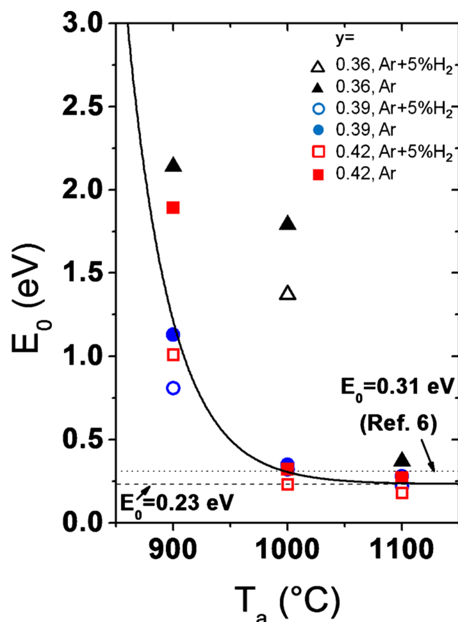

FIG. 5. (Color online) Annealing temperature dependence of E_0 for y =(0.36,0.39,0.42)—triangle, circle, and square, respectively. Empty (full) symbols corresponds for hydrogenated (nonhydrogenated) samples. The solid line is a guide for the eye.

size). Here, we observe that this energy dispersion becomes very small with decreasing T_a for which, according to the Raman data [Fig. 2, Tables I and II], Si-ncl become disordered and contribute to a relatively large volume fraction of amorphous Si. Concomitantly, the PL decay rate becomes high [Fig. 3(b)]. Possible reasons for these effects are, on one hand, the gradual suppression of the QC in disordered Si-ncl due to disorder induced exciton localization or decoherence [in an amorphous Si-ncl the electronic wave function coherence lengths may become as small as 1 nm,[17] i.e., significantly smaller than the typical Si-ncl sizes of 3–6 nm (Refs. 10 and 18)]. On the other hand, in amorphous Si-ncl, the nonradiative recombination rate is expected to increase due to the typical presence of Si dangling bonds, and may eventually dominate the total PL decay rate due to the large capture cross section of these defects.[19] According to Street,[20] the total PL rates for bulk a-Si:H are on the order of $\sim 10^5$ s^{-1} at 81 K. The larger PL rates of $\sim 5\times 10^5$ s^{-1} for our samples annealed at 900 °C are comparable to those measured by Irrera *et al.*[21] for Si-ncl prepared at the same annealing temperature. It is interesting to note that theoretical work by Allan *et al.*[22] for amorphous hydrogenated Si-ncl have predicted radiative rates on the same order of magnitude as those reported here, and attributed to disorder-induced breakdown of the k-conservation rule in the amorphous clusters in addition to the QC effect. Furthermore, the weak dependence on band-gap energy of the radiative rates for the amorphous Si-ncl (see Fig. 4 of Ref. 22) is in qualitative agreement with the high E_0 values obtained experimentally here for the samples annealed at 900 °C. This agreement is an indication that QC may still be a factor in the determination of the PL rates in the amorphous Si-ncl studied here.

A weak E_0 dependence on y is also observed for T_a =1100 °C (see Fig. 4). In this case, E_0 decreases slightly with increasing y, while the decay rate increases strongly. We propose that this is evidence for significant contributions of the so called "exciton hopping mechanism"[5] to the total decay rate. Higher Si content is known to yield larger Si-ncl mean size[10,18] and, as the present Raman data show [Fig. 2(b)], to larger Si-ncl density for fixed annealing conditions. Hence, exciton hopping between neighboring Si-ncl may be expected to be enhanced with increasing y.[5] The decrease in β with increasing Si content (see Fig. 4) strengthens the idea of increasing exciton hopping contributions.[4]

The deduced E_0 values for samples prepared under the different fabrication conditions considered in this work are summarized in Fig. 5, as a function of T_a. The solid line is a guide for the eye. For low T_a, E_0 values are relatively large for all samples and depend on the fabrication conditions. With increasing T_a these values decrease significantly and become almost independent of the fabrication conditions and roughly equal to the value predicted by Delerue *et al.*[6] and experimentally obtained by various studies.[3–6]

IV. CONCLUSIONS

The emission energy dependence of the PL decay rate at room temperature has been studied in various Si-ncl/Si oxide samples obtained by thermal annealing at various T_a in Ar and (Ar+5%H_2) of substoichiometric Si oxide layers of various Si contents. Raman data give evidence for the formation of Si-ncl within the Si oxide which are essentially amorphous for T_a=900 °C and crystalline for T_a=1000 and 1100 °C. Equation (1) is found to be fulfilled in all cases, with the characteristic E_0 value independent of fabrication conditions and in agreement with the previously reported value for T_a=1100 °C, but increasing and becoming dependent on fabrication conditions for lower T_a. The effects are suggested to be due to disorder induced localization and decoherence leading to the gradual suppression of QC and increasing nonradiative recombination rates in disordered and amorphous Si-ncl.

ACKNOWLEDGMENTS

We acknowledge financial support through the Inter-American Collaboration in Materials (CIAM) initiative, from the Brazilian Agencies CNPq and FAPESP, the Argentinean CONICET and The Academy of Sciences for the Developing World (TWAS). The work at McMaster University is supported by the Natural Sciences and Engineering Research Council (NSERC), the Canadian Institute for Photonic Innovation (CIPI) and the Centre for Photonics of Ontario Centres of Excellence, Inc.

[1] F. Iacona, G. Franzo, and C. Spinella, J. Appl. Phys. **87**, 1295 (2000).
[2] T. Shimizu-Iwayama, Y. Terao, A. Kamiya, and M. Takeda, Thin Solid Films **276**, 104 (1996).
[3] M. L. Brongersma, P. G. Kik, A. Polman, K. S. Min, and H. A. Atwater, Appl. Phys. Lett. **76**, 351 (2000).
[4] J. Derr, K. Dunn, D. Riabinina, F. Martin, M. Chaker, and F. Rosei, Physica E (Amsterdam) **41**, 668 (2009).
[5] L. Pavesi, J. Appl. Phys. **80**, 216 (1996).
[6] C. Delerue, G. Allan, C. Reynaud, O. Guillois, G. Ledoux, and F. Huisken, Phys. Rev. B **73**, 235318 (2006).

Author complimentary copy. Redistribution subject to AIP license or copyright, see http://jap.aip.org/jap/copyright.jsp

[7]L. Khriachtchev, T. Nikitin, R. Velagapudi, J. Lahtinen, and S. Novikov, Appl. Phys. Lett. **94**, 043115 (2009).
[8]M. Boudreau, M. Boumerzoug, P. Mascher, and P. E. Jessop, Appl. Phys. Lett. **63**, 3014 (1993).
[9]D. Comedi, O. H. Y. Zalloum, J. Wojcik, and P. Mascher, IEEE J. Sel. Top. Quantum Electron. **12**, 1561 (2006).
[10]D. Comedi, O. H. Y. Zalloum, E. A. Irving, J. Wojcik, and P. Mascher, J. Vac. Sci. Technol. A **24**, 817 (2006).
[11]Z.-X. Ma, X. B. Liao, G. L. Kong, and J. H. Chu, Chin. Phys. **9**, 309 (2000).
[12]D. Bermejo and M. Cardona, J. Non-Cryst. Solids **32**, 405 (1979).
[13]K. W. Adu, H. R. Gutierrez, U. J. Kim, G. U. Sumanasekera, and P. C. Eklund, Nano Lett. **5**, 409 (2005).
[14]C. Smit, R. A. C. M. M. van Swaaij, H. Donker, A. M. H. N. Petit, W. M. M. Kessels, and M. C. M. van de Sanden, J. Appl. Phys. **94**, 3582 (2003).
[15]C. Garcia, B. Garrido, P. Pellegrino, R. Ferre, J. A. Moreno, J. R. Morante, L. Pavesi, and M. Cazzanelli, Appl. Phys. Lett. **82**, 1595 (2003).
[16]G. Davies, Phys. Rep. **176**, 83 (1989).
[17]R. A. Street, *Hydrogenated Amorphous Silicon* (Cambridge University Press, Cambridge, UK, 1991).
[18]D. Comedi, O. H. Y. Zalloum, E. A. Irving, J. Wojcik, T. Roschuk, M. J. Flynn, and P. Mascher, J. Appl. Phys. **99**, 023518 (2006).
[19]M. Lannoo, C. Delerue, and G. Allan, J. Lumin. **70**, 170 (1996).
[20]R. A. Street, Adv. Phys. **30**, 593 (1981).
[21]A. Irrera, F. Iacona, I. Crupi, C. D. Presti, G. Franzo, C. Bongiorno, D. Sanfilippo, G. Di Stefano, A. Piana, P. G. Fallica, A. Canino, and F. Priolo, Nanotechnology **17**, 1428 (2006).
[22]G. Allan, C. Delerue, and M. Lannoo, Phys. Rev. Lett. **78**, 3161 (1997).

Author complimentary copy. Redistribution subject to AIP license or copyright, see http://jap.aip.org/jap/copyright.jsp